Nanoscale

PAPER

View Article Online
View Journal | View Issue

Cite this: *Nanoscale*, 2014, **6**, 1629

Versatile multi-functionalization of protein nanofibrils for biosensor applications†

L. Sasso,*[abc] S. Suei,[ad] L. Domigan,[abce] J. Healy,[bc] V. Nock,[abf] M. A. K. Williams[adg] and J. A. Gerrard*[abch]

Protein nanofibrils offer advantages over other nanostructures due to the ease in their self-assembly and the versatility of surface chemistry available. Yet, an efficient and general methodology for their post-assembly functionalization remains a significant challenge. We introduce a generic approach, based on biotinylation and thiolation, for the multi-functionalization of protein nanofibrils self-assembled from whey proteins. Biochemical characterization shows the effects of the functionalization onto the nanofibrils' surface, giving insights into the changes in surface chemistry of the nanostructures. We show how these methods can be used to decorate whey protein nanofibrils with several components such as fluorescent quantum dots, enzymes, and metal nanoparticles. A multi-functionalization approach is used, as a proof of principle, for the development of a glucose biosensor platform, where the protein nanofibrils act as nanoscaffolds for glucose oxidase. Biotinylation is used for enzyme attachment and thiolation for nanoscaffold anchoring onto a gold electrode surface. Characterization *via* cyclic voltammetry shows an increase in glucose-oxidase mediated current response due to thiol–metal interactions with the gold electrode. The presented approach for protein nanofibril multi-functionalization is novel and has the potential of being applied to other protein nanostructures with similar surface chemistry.

Received 28th October 2013
Accepted 15th November 2013

DOI: 10.1039/c3nr05752f

www.rsc.org/nanoscale

1. Introduction

Amyloid fibrils are insoluble biological nanostructures formed *via* self-assembly of proteins. The self-assembly of mature fibrils has been extensively studied and this process varies slightly with the source protein building block. Although several mechanisms have been proposed,[1] the most accepted theory relies on partial un-folding of the protein monomers[2] and the formation of intermediates which undergo nucleation-dependent polymerization.[3] Amyloid fibrils have a characteristic β-sheet rich conformation,[4,5] with a rigid internal order resulting in distinctive properties such as high strength, stability and high aspect-ratio dimensions,[6,7] with widths in the range of 2–10 nm (ref. 8) and lengths from 1 up to 10 μm (see Fig. 1). The variety in amino acid sequences available within the protein

[a]*MacDiarmid Institute for Advanced Materials and Nanotechnology, Wellington 6140, New Zealand. E-mail: luigi.sasso@canterbury.ac.nz*

[b]*Biomolecular Interaction Centre, University of Canterbury, Christchurch 8140, New Zealand*

[c]*School of Biological Sciences, University of Canterbury, Christchurch 8140, New Zealand*

[d]*Institute of Fundamental Sciences, Massey University, Palmerston North 4442, New Zealand*

[e]*Department of Biomedical Engineering, Tufts University, Medford 02155, MA, USA*

[f]*Department of Electrical and Computer Engineering, University of Canterbury, 8140, New Zealand*

[g]*Riddet Institute, Massey University, Palmerston North 4442, New Zealand*

[h]*Callaghan Innovation Research Ltd, Lower Hutt 5040, New Zealand. E-mail: juliet.gerrard@canterbury.ac.nz*

† Electronic supplementary information (ESI) available: Cyclic voltammetry characterization of biosensor platforms including bare Au electrodes (Fig. S1), biosensor response to various glucose concentrations (Fig. S2), and AFM roughness measurements due to WPNF modifications (Fig. S3). See DOI: 10.1039/c3nr05752f

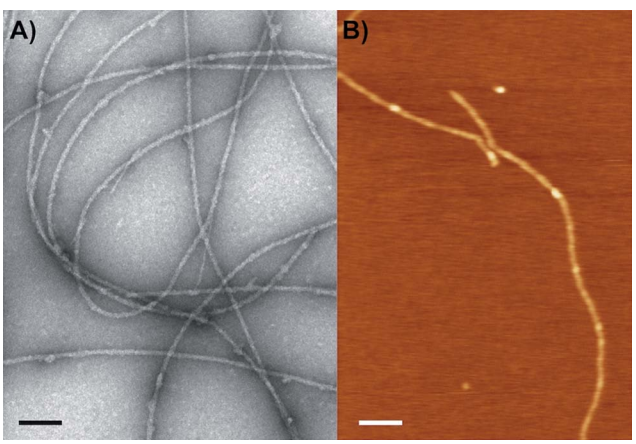

Fig. 1 (a) TEM image of whey protein nanofibrils (scale bar corresponds to 100 nm); (b) AFM image of whey protein nanofibrils (scale bar is 500 nm).

building blocks offer anchoring points along the nanostructure's surface, allowing for the functionalization of amyloid fibrils with components useful in the application of this nanoscaffold.[9–13] This affords some advantages over similarly sized structures, such as carbon nanotubes, where the introduction of more than one type of chemical functionality to the surface remains a challenge.[14]

There are a myriad of protein sources available which can undergo fibril formation, such as insulin,[15] ovalbumin,[16] lysozyme,[17] eye lens crystallins,[18] fungal hydrophobins,[19] soy[20] and whey proteins.[21] Whey proteins are of particular interest for fibril formation mainly because of their inexpensiveness and availability, since whey protein isolates (WPIs) are a common byproduct of the dairy industry. The major components of WPIs are β-lactoglobulin, α-lactalbumin and serum albumin.[22] Aside from the wide use of WPIs in the food industry as functional materials in dairy products, mainly because of their gelation abilities,[23–25] whey protein nanofibrils (WPNFs) have been widely studied and characterized as nanomaterials.[26–33] The current literature focuses mainly on understanding the mechanism of formation of these nanofibrils, and only a few studies exist about the post-assembly applications of WPNFs as nanomaterials.[34–36] Research in the latter area has been restricted to peptide-based nanostructures,[37–41] which are inherently much less stable bionanomaterials than amyloid fibrils, particularly for devices that may be exposed to aqueous solvents.[42] Modification of biological nanostructures has also generally been restricted to addition of a single moiety.[9–13,43–45] The ability to add more than one entity to a nanoscaffold surface, still a hurdle to overcome in the field,[13] opens up many new applications.[46] One of the major challenges that has limited the application of WPNFs to date is obtaining a reliable control over the nanostructures' post-assembly modifications, such as the attachment of relevant compounds to their surface, in order to specifically utilize WPNFs as nanoscaffold materials for broader applications, for example in the electronic or biosensing field.

We demonstrate here a reliable, versatile method for the multi-functionalization of WPNFs, utilizing chemical anchoring points present on the surface of the bionanostructures.

2. Experimental

2.1. Chemicals and materials

Whey protein isolate (WPI) 895 was obtained from Fonterra Co-operative Group (Auckland, New Zealand). Biotin 3-sulfo-*N*-hydroxysuccinimide ester sodium salt (Biotin), 2-iminothiolane hydrochloride (Traut's Reagent), *o*-phthaldialdehyde (OPA), 5,5′-dithio-bis(2-nitrobenzoic acid) (Ellman's Reagent), 2-mercaptoethanol, sodium borate, sodium phosphate and ethylenediaminetetraacetic acid (EDTA) were purchased from Sigma Aldrich (Steinheim, Germany). Methanol was obtained from Ajax Finechem Pty Ltd (Taren Point, Australia) and hydroxymethyl ferrocene (FcOH) from AlfaAesar (Ward Hill, MA, USA). Streptavidin coated glucose oxidase (GOx) was purchased from Fitzgerald Industries (Acton, MA, USA), streptavidin coated quantum dots (Qdot® 655) from Molecular Probes, Inc. (Eugene, OR, USA), uranyl acetate from BDH Chemicals Ltd (Kingston upon Hull, UK) and D(+)-glucose anhydrous from VWR International BVBA (Leuven, Belgium). Gold nanoparticles 10–40 μm in diameter were synthesized in-house. All solutions used in this work were prepared using filtered (0.22 μm) ultrapure water from a Milli-Q® water purification system from Millipore Corporation (Billerica, MA, USA).

2.2. Preparation of WPNFs[33]

Aqueous solution of whey protein isolate (10 mg mL^{-1}) was prepared and stirred for 10 min. The pH was adjusted to 2.0 with addition of 1.0 M HCl and 0.1 M KOH using a pH probe (Denver Instrument, Bohemia, NJ, USA). The solutions were left overnight at 4 °C while stirring, and then heated to 80 °C for 20–22 hours in a dry bath heater (Labnet International Inc., Woodridge, NJ, USA). After cooling for 10 min on ice, the resulting WPNF suspensions were kept at room temperature for at least 1 week before proceeding with the experiments.

2.3. TEM[47] and AFM[8] characterization

Before preparing the TEM grids, the concentrations of the WPNF suspensions were adjusted to 0.1 mg mL^{-1}. Each grid was exposed to 20 μL of sample for 1 min, then to 20 μL of water for 20 s thrice, and finally to 20 μL of uranyl acetate (1%). A FEI Morgagni 268 TEM was used (FEI, Hillsboro, OR, USA). For the AFM characterization, 10 μL of WPNF suspension (0.1 mg mL^{-1}) were loaded onto a freshly cleaved mica and air-dried before imaging. AFM imaging was carried out on a FlexAFM from Nanosurf (Scitech, Victoria, Australia) and a NanoScopeIIIa (Bruker, Santa Barbara, CA, USA) in tapping mode using Tap190Al-G and Tap300AI-G cantilevers with a nominal spring constant of 40 N m^{-1} and a nominal tip radius <10 nm from Budget Sensors (Innovative Solutions Bulgaria Ltd., Sofia, Bulgaria).

2.4. Functionalization of WPNFs

Biotinylation of WPNFs was achieved by adding an aqueous biotin stock solution of 10 mg mL^{-1} to an undiluted WPNF suspension (with original protein concentration of 10 mg mL^{-1}) and thiolation similarly by addition of Traut's reagent stock solution (10 mg mL^{-1}) to a WPNF suspension (10 mg mL^{-1}). For the multi-functionalization, biotin and Traut's reagent were added in excess at the same time in ratios of 1 mg mg^{-1} WPNF for each reagent. Samples were incubated at room temperature for 2 hours. A streptavidin-coated glucose oxidase solution (1 mg mL^{-1}) was added to the biotinylated WPNF suspension to a final concentration of 40 μg mL^{-1}. Streptavidin-coated quantum dots were similarly added to a final concentration of 10 nM.

2.5. Spectroscopy-based assays

For the OPA assay,[48] 300 μL of OPA solution were added to 50 μL of each sample (biotinylated WPNF suspensions, diluted to 1 mg mL^{-1}). The OPA solution was prepared by first dissolving 40 mg of OPA in 1 mL methanol, then adding this to 49 mL of buffer containing: 25 mL sodium borate (0.1 M), 100 μL 2-mercaptoethanol and 23.9 mL water. After 2 min of incubation at room temperature under dark conditions, the

fluorescence measurements were carried out at 340 nm (emission at 455 nm). Fluorescence measurements were normalized to the average maximum fluorescence, obtained at 0 mg added biotin. For Ellman's assay,[49] 5 μL of Ellman's reagent solution (4 mg of Ellman's reagent in 1 mL reaction buffer containing 0.1 M sodium phosphate and 1 mM EDTA) was added to 250 μL reaction buffer and 25 μL of each sample (thiolated WPNF suspensions, diluted to 1 mg mL^{-1}). After a 15 min incubation at room temperature and dark conditions, the absorbance measurements were carried out at 412 nm. A SpectraMax M5 Multi-Mode Microplate Reader and clear flat-bottom 96 microwell plates were used for the work (Molecular Devices, Sunnyvale, CA, USA). Each data point is representative of averages from triplicate samples and 4 measurements for each, with subtracted blanks.

2.6. Electrochemical biosensor characterization[50]

Electrochemical measurements were carried out using a potentiostat from eDAQ Pty Ltd (Denistone East, Australia) and commercial screen-printed gold electrodes (C223AT) with an appropriate connector (DRP-CAC) from DropSens (Oviedo, Spain). Deposition of functionalized WPNFs on the electrode surfaces was done by pipetting 2 μL of a WPNF suspension (2 mg mL^{-1}) onto the working electrode and by drying the surface for 1 hour at 37 °C. Electrodes were dipped into mediator solutions (FcOH, 1.5 mM) with or without glucose (500 mM) immediately prior to experiments.

3. Results and discussion

3.1. Functionalization

The nanoscale properties of WPNFs provide them with a large surface-to-volume ratio allowing for the possibility of a high functionalization packing density. This work exploits the variety of chemical moieties present on the surface of the WPNFs, focusing on two approaches to chemical surface modification: biotinylation and thiolation.

The biotin–streptavidin interaction is known as one of the strongest bonds in nature.[51,52] This approach to WPNF functionalization therefore yields a particularly stable anchor point and also provides flexibility in functionalization, since many commercially available streptavidin-conjugated components can be found. The biotinylation of WPNFs was achieved *via* a commercially available succinimide-based biotin conjugate that targets the primary amine groups present on the surface of the WPNFs.

The cross-linking of biotin to the fibrils' free amine groups was characterized using the *o*-phthaldialdehyde (OPA) assay.[48,53] As shown in Fig. 2A, an increase in the biotin concentration decreases the amount of free amine groups on the WPNFs' surface, as expected. Once the surface of the WPNFs has been biotinylated, the addition of streptavidin-coated components allows for the functionalization of the WPNFs with many different elements, such as quantum dots (see Fig. 3), useful in fluorescence visualization of the structures, and bioanalytically relevant molecules like enzymes such as glucose oxidase (GOx) (see Fig. 4A).

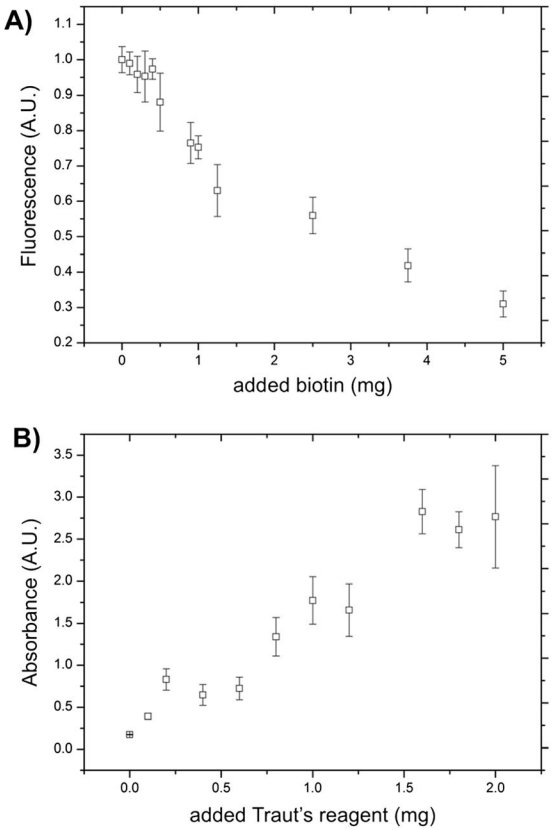

Fig. 2 (a) OPA and (b) Ellman's reaction assays on functionalized WPNFs. Horizontal axes represent mg of added biotin and Traut's reagent per mg WPNF.

Thiolation is a widely used method for supplementing or exposing free sulfhydryl groups on a surface.[55] The method has found many applications, from increasing the antimicrobial

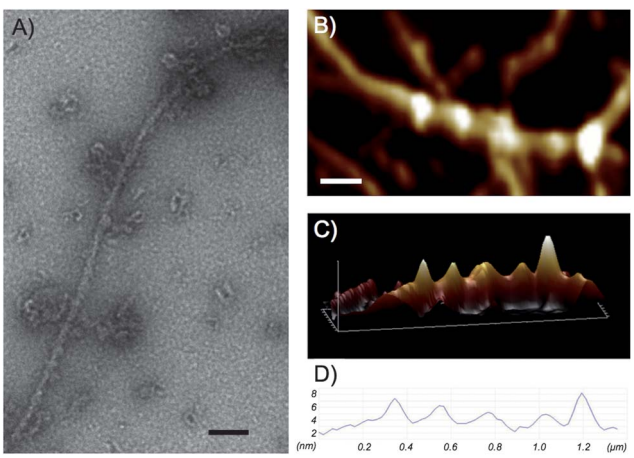

Fig. 3 (a) TEM image of a quantum dot-functionalized WPNF (scale bar corresponds to 50 nm); (b) AFM height image (scale bar is 200 nm), (c) 3D display and (d) cross-section of a quantum dot-functionalized WPNF, showing the characteristic repeats of quantum dots (6–8 nm in height) on the WPNF. Discrepancies in fibril widths/heights between TEM and AFM analyses can be ascribed to effects of surface-type differences on protein nanostructure–substrate adsorption interactions.[54]

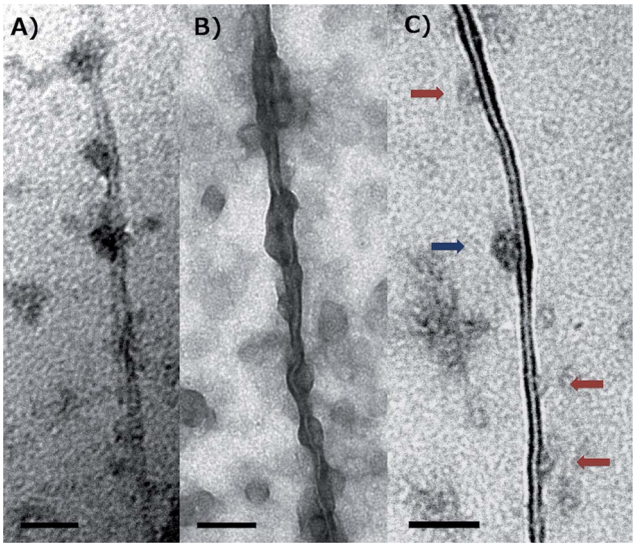

Fig. 4 TEM images of WPNFs functionalized with (a) glucose oxidase, (b) gold nanoparticles and (c) both glucose oxidase (blue arrow) and gold nanoparticles (red arrows). Scale bars correspond to 50 nm.

activity of peptides[56] to providing a strategy for the metallization of nanostructures[40] and the attachment of biological materials onto gold surfaces[39,43,57] and metal nanoparticles,[58] since thiols are known for their affinity to metals.[59] A reliable method for the thiolation of primary amines is *via* spontaneous reaction with Traut's reagent.[55]

The thiolation of WPNFs with Traut's reagent, and therefore the formation of thiol groups on their surface, was characterized *via* Ellman's assay, an absorbance-based method for sulfhydryl quantification.[49] The assay demonstrated an increasing trend in the amount of free sulfhydryls with increasing amount of Traut's reagent used (see Fig. 2B). Thiolated WPNFs were then used for the attachment of gold nanoparticles (see Fig. 4B).

The two functionalization strategies discussed in this work can also be used together to provide a method for attachment of different components onto the same nanofibril scaffold. By providing both biotin and thiol groups on their surface, WPNFs can be functionalized both with enzymes and metal nanoparticles (see Fig. 4C). This approach will be useful in the patterning of bionanostructures onto surfaces[43] and in their application to biosensor platforms,[60] especially in regard to dual-enzyme biosensor systems.[61] The side-chain chemistry of other amino acids can also be brought into play, providing an extensive repertoire of potential anchoring points.

3.2. Biosensor application

The advantage of the multi-functionalization method was demonstrated by immobilizing enzymes onto a WPNF nanoscaffold using one anchoring moiety and further attaching these functionalized components onto electrodes with another, for use in electrochemical biosensing. The immobilization technique used had an augmented effect on the detection efficiency, and the use of nanoscaffolds is expected to increase the overall sensitivity and stability of enzymatic biosensors.[62]

A glucose biosensor platform was constructed using GOx-functionalized WPNFs as nanoscaffolds for enzyme immobilization onto screen-printed gold electrodes (see Fig. 5A). Cyclic voltammetry was used to characterize the biosensor response to glucose, using a ferrocene derivative as a mediator (see Fig. 5B). Several variations of this platform were tested, comparing the current responses to glucose for different immobilization methods: (i) enzyme adsorption onto the gold electrode surface, with no use of the WPNF nanoscaffold (Au/GOx), (ii) physical adsorption of enzyme-functionalized WPNFs on the electrode surface (Au/WPNF–GOx), and (iii) surface anchoring of enzyme-functionalized WPNFs *via* thiol–metal interactions (Au/WPNF–GOx–SH). No change in response due to the presence of glucose in the ferrocene mediator solution was detected for bare Au electrodes, where no enzyme was present (see ESI Fig. S1†).

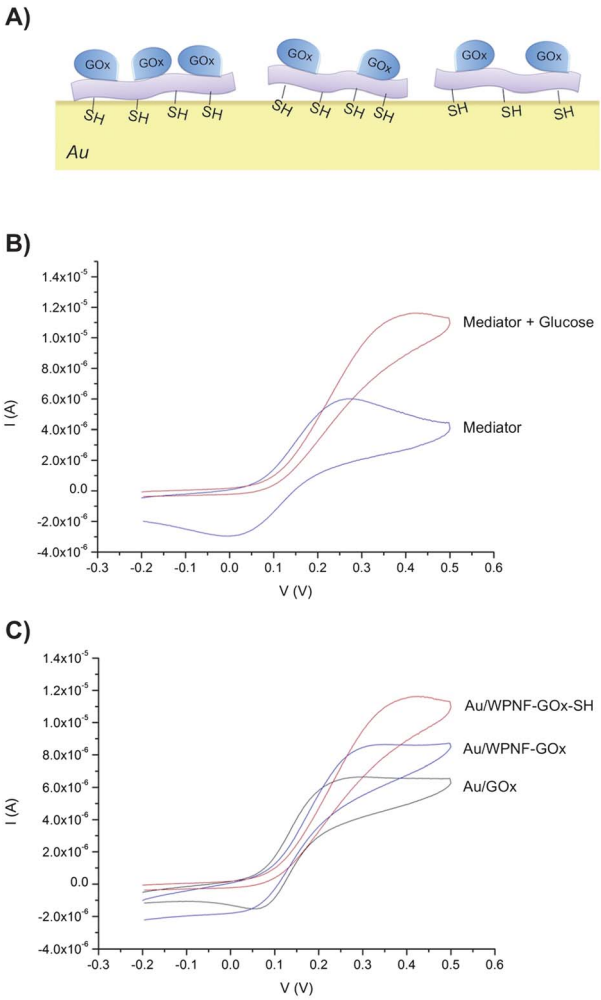

Fig. 5 (a) Schematic of biosensor platform based on GOx- and SH-functionalized WPNFs. (b) Typical cyclic voltammograms of the platform's response to glucose (500 mM) in a FCOH mediator (1.5 mM) (red) and to the mediator alone (blue). (c) Comparison of glucose responses for different enzyme immobilization methods: adsorption onto a bare gold electrode (Au/GOx), GOx-functionalized WPNF deposition (Au/WPNF–GOx), and multi- GOx- and SH-functionalized WPNF deposition (Au/WPNF–GOx–SH). Potential sweep rates are 100 mV s^{-1}, using an Au counter and Ag reference electrode.

Although the glucose concentration used in the initial characterization was in excess (500 mM), a variation in response to different glucose concentrations for the biosensor platform (iii) was observed (see ESI Fig. S2†). Typical voltammograms (see Fig. 5C) exhibit an increase in anodic peak current response when using the WPNF nanoscaffolds (ii), compared to simple enzyme adsorption (i), showing an increase in enzyme immobilization due to the large surface-to-volume ratio of the WPNF nanoscaffold. The anodic peak currents are even larger when using the multi-functionalization approach including thiolation of the WPNFs (iii), suggesting an increase in WPNF anchoring to the gold surface due to the thiol–metal interactions when compared to physical adsorption only. Additionally, this trend in nanoscaffold anchoring is supported by a potential shift of the anodic current peaks (Fig. 5C), reflecting an increase in mass transport limitations when going from (i) to (ii) to (iii). The effects of the thiol functionalization on WPNF anchoring to the electrode surface are also indicated by an increase in electrode roughness when compared with non-functionalized WPNFs, assessed by AFM-based measurements (see ESI Fig. S3†).

4. Conclusions

In summary, we have shown in this work a novel, reliable and versatile approach for the single and multi-functionalization of WPNFs. The nanostructures were functionalized with several components utilizing a biotinylation and a thiolation method. Biochemical and electrochemical characterization, along with TEM and AFM visualizations, gave an insight into the functionalization methods and validated their performance.

The cross-linking of biotin to the WPNFs' primary amines was biochemically characterized *via* OPA assay, showing a decrease in amine availability with increasing biotin addition. Using biotin–streptavidin interactions, the WPNFs were functionalized with fluorescent quantum dots and GOx enzymes.

The thiolation of the WPNFs *via* Traut's reagent's reaction with the nanostructures' primary amines was achieved and characterized *via* Ellman's assay. Thiolation of the nanofibrils' surface allowed for the attachment of gold nanoparticles to the bionanostructures, as well as provided a method for anchoring them to gold surfaces.

The original multi-functionalization method developed, based on parallel biotinylation and thiolation, was used to anchor quantum dots and gold nanoparticles onto the same individual protein nanofibrils. The multi-functionalization method was also used to create an electrochemical enzymatic biosensor platform comprising of GOx-functionalized, thiolated WPNFs. An electrochemical characterization *via* cyclic voltammetry showed an increase in current response when using the multi-functionalization method, promising an increase in sensitivity of the biosensor platform.

The future goals of this research will include extending this versatile multi-functionalization method to other protein nanostructures with similar surface chemistries. This work provides a useful tool for the manipulation and functionalization of biological nanostructures, and specifically for their application in the biosensor field.

Acknowledgements

This work is supported by the MacDiarmid Institute for Advanced Materials and Nanotechnology. Partial funding was obtained *via* contract number UOCX1209 from the New Zealand Ministry of Business, Innovation and Employment. The authors would like to thank Prof. Alison Downard (Dept. of Chemistry, University of Canterbury) for access to the potentiostat used in this work.

References

1 M. Groenning, S. Frokjaer and B. Vestergaard, *Curr. Protein Pept. Sci.*, 2009, **10**, 509.
2 Q. X. Hua and M. A. Weiss, *J. Biol. Chem.*, 2004, **279**, 21449.
3 J. D. Harper and P. T. Lansbury, *Annu. Rev. Biochem.*, 1997, **66**, 385.
4 F. Chiti and C. M. Dobson, *Annu. Rev. Biochem.*, 2006, **75**, 333.
5 M. Fandrich, *Cell. Mol. Life Sci.*, 2007, **64**, 2066.
6 O. G. Jones and R. Mezzenga, *Soft Matter*, 2012, **8**, 876.
7 L. J. Domigan, J. P. Healy, S. J. Meade, R. J. Blaikie and J. A. Gerrard, *Biopolymers*, 2012, **97**, 123.
8 J. Adamcik, J. Jin-Mi, J. Flakowski, P. De Los Rios, G. Dietler and R. Mezzenga, *Nat. Nanotechnol.*, 2010, **5**, 423.
9 N. Hendler, B. Belgorodsky, E. D. Mentovich, S. Richter, L. Fadeev and M. Gozin, *Adv. Funct. Mater.*, 2012, **22**, 3765.
10 S. M. Pilkington, S. J. Roberts, S. J. Meade and J. A. Gerrard, *Biotechnol. Prog.*, 2010, **26**, 93.
11 C. Muller, R. Jansson, A. Elfwing, G. Askarieh, R. Karlsson, M. Hamedi, A. Rising, J. Johansson, O. Inganas and M. Hedhammar, *J. Mater. Chem.*, 2011, **21**, 2909.
12 Q. Tang, N. Solin, J. Lu and O. Inganas, *Chem. Commun.*, 2010, **46**, 4157.
13 D. N. Woolfson and Z. N. Mahmoud, *Chem. Soc. Rev.*, 2010, **39**, 3764.
14 K. M. Lee, L. C. Li and L. M. Dai, *J. Am. Chem. Soc.*, 2005, **127**, 4122.
15 C. Ha and C. B. Park, *Biotechnol. Bioeng.*, 2005, **90**, 848.
16 F. G. Pearce, S. H. Mackintosh and J. A. Gerrard, *J. Agric. Food Chem.*, 2007, **55**, 318.
17 R. Mishra, K. Sorgjerd, S. Nystrom, A. Nordigarden, Y. C. Yu and P. Hammarstrom, *J. Mol. Biol.*, 2007, **366**, 1029.
18 J. Healy, K. Wong, E. B. Sawyer, C. Roux, L. Domigan, S. L. Gras, M. Sunde, N. G. Larsen, J. Gerrard and M. Vasudevamurthy, *Biopolymers*, 2012, **97**, 595.
19 V. K. Morris and M. Sunde, in *Protein Nanotechnology*, ed. J. A. Gerrard, Humana Press, New York, USA, 2nd edn, 2013, ch. 7.
20 C. H. Tang, S. S. Wang and Q. R. Huang, *Food Res. Int.*, 2012, **46**, 229.
21 S. G. Bolder, H. Hendrickx, L. M. C. Sagis and E. van der Linden, *J. Agric. Food Chem.*, 2006, **54**, 4229.
22 C. Holt, D. McPhail, I. Nevison, T. Nylander, J. Otte, R. H. Ipsen, R. Bauer, L. Ogendal, K. Olieman, K. G. de

Kruif, J. Leonil, D. Molle, G. Henry, J. L. Maubois, M. D. Perez, P. Puyol, M. Calvo, S. M. Bury, G. Kontopidis, I. McNae, L. Sawyer, L. Ragona, L. Zetta, H. Molinari, B. Klarenbeek, M. J. Jonkman, J. Moulin and D. Chatterton, *Int. J. Food Sci. Technol.*, 1999, **34**, 543.

23 S. G. Bolder, H. Hendrickx, L. M. C. Sagis and E. Van der Linden, *Appl. Rheol.*, 2006, **16**, 258.

24 J. T. de Faria, V. P. R. Minim and L. A. Minim, *Food Hydrocolloids*, 2013, **32**, 64.

25 S. M. Loveday, M. A. Rao, L. K. Creamer and H. Singh, *J. Food Sci.*, 2009, **74**, R47.

26 S. M. Loveday, J. Su, M. A. Rao, S. G. Anema and H. Singh, *J. Agric. Food Chem.*, 2012, **60**, 5229.

27 S. M. Loveday, J. Su, M. A. Rao, S. G. Anema and H. Singh, *Int. Dairy J.*, 2012, **26**, 133.

28 S. M. Loveday, X. L. Wang, M. A. Rao, S. G. Anema, L. K. Creamer and H. Singh, *Int. Dairy J.*, 2010, **20**, 571.

29 S. M. Loveday, X. L. Wang, M. A. Rao, S. G. Anema and H. Singh, *J. Agric. Food Chem.*, 2011, **59**, 8467.

30 S. M. Loveday, X. L. Wang, M. A. Rao, S. G. Anema and H. Singh, *Food Hydrocolloids*, 2012, **27**, 242.

31 C. A. Hettiarachchi, L. D. Melton, J. A. Gerrard and S. M. Loveday, *Biomacromolecules*, 2012, **13**, 2868.

32 S. M. Loveday, J. H. Su, M. A. Rao, S. G. Anema and H. Singh, *J. Agric. Food Chem.*, 2012, **60**, 5229.

33 S. M. Loveday, J. Su, M. A. Rao, S. G. Anema and H. Singh, *Biomacromolecules*, 2011, **12**, 3780.

34 S. Bolisetty, J. Adamcik, J. Heier and R. Mezzenga, *Adv. Funct. Mater.*, 2012, **22**, 3424.

35 C. Li, J. Adamcik and R. Mezzenga, *Nat. Nanotechnol.*, 2012, **7**, 421.

36 C. Li, S. Bolisetty and R. Mezzenga, *Adv. Mater.*, 2013, **25**, 3694.

37 L. Adler-Abramovich, M. Badihi-Mossberg, E. Gazit and J. Rishpon, *Small*, 2010, **6**, 825.

38 R. J. Brea, C. Reiriz and J. R. Granja, *Chem. Soc. Rev.*, 2010, **39**, 1448.

39 B. W. Park, R. Zheng, K. A. Ko, B. D. Cameron, D. Y. Yoon and D. S. Kim, *Biosens. Bioelectron.*, 2012, **38**, 295.

40 J. I. Yeh, A. Lazareck, J. H. Kim, J. Xu and S. Du, *Biosens. Bioelectron.*, 2007, **23**, 568.

41 C. Valery, F. Artzner and M. Paternostre, *Soft Matter*, 2011, **7**, 9583.

42 K. B. Andersen, J. Castillo-Leon, M. Hedstrom and W. E. Svendsen, *Nanoscale*, 2011, **3**, 994.

43 I. A. Banerjee, L. Yu, R. I. MacCuspie and H. Matsui, *Nano Lett.*, 2004, **4**, 2437.

44 O. Carny, D. E. Shalev and E. Gazit, *Nano Lett.*, 2006, **6**, 1594; E. C. Cho, J.-W. Choi, M. Lee and K.-K. Koo, *Colloids Surf., A*, 2008, **313–314**, 95.

45 J. K. Raynes, F. G. Pearce, S. J. Meade and J. A. Gerrard, *Biotechnol. Prog.*, 2011, **27**, 360.

46 M. E. Pearce, J. B. Melanko and A. K. Salem, *Pharm. Res.*, 2007, **24**, 2335.

47 W. van Grondelle, C. L. Iglesias, E. Coll, F. Artzner, M. Paternostre, F. Lacombe, M. Cardus, G. Martinez, M. Montes, R. Cherif-Cheikh and C. Valery, *J. Struct. Biol.*, 2007, **160**, 211.

48 M. Roth, *Anal. Chem.*, 1971, **43**, 880.

49 C. K. Riener, G. Kada and H. Gruber, *Anal. Bioanal. Chem.*, 2002, **373**, 266.

50 J. Lehr, B. E. Williamson, F. Barriere and A. Downard, *Bioelectrochemistry*, 2010, **79**, 142.

51 A. Holmberg, A. Blomstergren, O. Nord, M. Lukacs, J. Lundeberg and M. Uhlen, *Electrophoresis*, 2005, **26**, 501.

52 O. H. Laitinen, V. P. Hytonen, H. R. Nordlund and M. S. Kulomaa, *Cell. Mol. Life Sci.*, 2006, **63**, 2992.

53 A. S. Cabeza, Y. M. Martinez, C. M. Legua and P. C. Falco, *Anal. Bioanal. Chem.*, 2003, **376**, 918.

54 N. K. Dutta, N. R. Choudhury, M. Y. Truong, M. Kim, C. M. Elvin and A. J. Hill, *Biomaterials*, 2009, **30**, 4868.

55 R. R. Traut, A. Bollen, T. T. Sun, J. W. B. Hershey, J. Sundberg and L. R. Pierce, *Biochemistry*, 1973, **12**, 3266.

56 N. Wiradharma, M. Khan, L. K. Yong, C. A. Hauser, S. V. Seow, S. Zhang and Y. Y. Yang, *Biomaterials*, 2011, **32**, 9100.

57 C. Ananthanawat, T. Vilaivan and V. P. Hoven, *Sens. Actuators, B*, 2009, **137**, 215.

58 A. M. Alkilany, S. E. Lohse and C. Murphy, *Acc. Chem. Res.*, 2013, **46**, 650.

59 R. S. Hu, S. T. Liu, T. Zhu, Z. F. Liu, X. H. Huang and H. Z. Huang, *Acta Biochim. Biophys. Sin.*, 1999, **15**, 961.

60 M. Yemini, M. Reches, J. Rishpon and E. Gazit, *Nano Lett.*, 2005, **5**, 183.

61 M. Ammam and J. Fransaer, *Sens. Actuators, B*, 2010, **148**, 583.

62 A. Sassolas, L. J. Blum and B. D. Leca-Bouvier, *Biotechnol. Adv.*, 2012, **30**, 489.

